Leaf economic and hydraulic divergences underpin ecological differentiation in the Bromeliaceae

Running title: Ecological differentiation in the Bromeliaceae

Jamie Males* & Howard Griffiths

Department of Plant Sciences, University of Cambridge, Downing Street, Cambridge, CB2 3EA, UK

*Author for correspondence

Email: jom23@cam.ac.uk; Telephone: +44 (0)1223 330218

Summary statement

The bromeliads are one of the most diverse plant families of the American tropics, and recognised as a model system for the study of evolutionary ecology and physiology. We show that divergences in key leaf traits can explain the differentiation of ecophysiological strategies among the major functional types, with important ramifications for our understanding of the evolutionary diversification of this extraordinary group of plants.

Abstract

Leaf economic and hydraulic theory have rarely been applied to the ecological differentiation of speciose herbaceous plant radiations. The role of character trait divergences and network reorganisation in the differentiation of the functional types in the megadiverse Neotropical Bromeliaceae was explored by quantifying a range of leaf economic and hydraulic traits in 50 diverse species. Functional types, which are defined by combinations of C_3 or CAM photosynthesis, terrestrial or epiphytic habits, and non-specialised, tank-forming or atmospheric morphologies, segregated clearly in trait space. Most classical leaf economic relationships were supported, but they were weakened by the presence of succulence. Functional types differed in trait-network architecture, suggesting that rewiring of trait-networks caused by innovations in habit and photosynthetic pathway is an important aspect of ecological differentiation. The hydraulic data supported the coupling of leaf hydraulics and gas exchange, but not the hydraulic safety vs. efficiency hypothesis, and hinted at an important role for the extra-xylary compartment in the control of bromeliad leaf hydraulics. Overall, our findings highlight the fundamental importance of structure-function relationships in the generation and maintenance of ecological diversity.

Keywords:

Bromeliaceae, leaf economics, leaf hydraulics, water relations, leaf anatomy, ecological differentiation, adaptive radiation

Introduction

[FIGURE 1]

The Neotropical Bromeliaceae is a highly diverse monocotyledonous family of some 3,500 species (Butcher & Gouda, 2016). A number of key innovations have been identified in the Bromeliaceae (Givnish et al., 2014), among which are absorptive foliar trichomes that facilitate the uptake of water and minerals, Crassulacean acid metabolism (CAM), epiphytism, and the tank growth form, in which a rosette of leaves forms a reservoir to trap water and leaf-litter. These innovations have shaped the evolutionary history of the bromeliad family, facilitating increased independence from the growth substrate and the invasion of varied environmental niches. Characteristic combinations of innovations can be used to define a series of ecologically distinctive functional types that have long been recognised (Fig. 1; scheme adapted from Pittendrigh, 1948). C_3 terrestrials range from mesophytic to somewhat xerophytic, while classic succulent xerophytes are found among the CAM terrestrials. C_3 tank-epiphytes are most abundant in relatively mesic canopy microhabitats, whereas most CAM tank-epiphytes tolerate higher exposure (Pittendrigh, 1948; Benzing, 2000). Meanwhile CAM atmospheric epiphytes occur in the most extreme microhabitats, using pulses of occult precipitation to maintain water balance. Until now, no quantitative analyses have explored how differences in leaf economic and hydraulic traits, and the architecture of the conceptual network of correlations that connects them (hereafter 'trait-network'), relate to ecological differentiation in the Bromeliaceae.

Leaf economic theory holds that fundamental developmental and physiological constraints limit the region of leaf trait hyperspace occupied during plant evolution (Reich et al., 1997, 1999; Wright et al., 2004, 2005; Donovan et al., 2011; Vasseur et al., 2012; Díaz et al., 2016). The core leaf economic traits, photosynthetic capacity (A_{max}), respiration rate (R), leaf nitrogen content (N_{leaf}), leaf phosphorus content (P_{leaf}), leaf mass per unit area (LMA), and leaf lifespan (LL), show strong coordination across the plant kingdom. Although leaf economic theory has focussed principally on covariation in a limited set of core traits, efforts have been made to extend the approach to consider other leaf traits, including leaf shape and size (Niinemets et al., 2007a), leaf hydraulics (Niinemets et al., 2007b; Sack et al., 2013), leaf defences (Mason & Donovan, 2015a), and genome and cell size (Beaulieu et al., 2007; Brodribb et al., 2013). The relationships between gas exchange, hydraulic conductance and hydraulic vulnerability are of particular interest because of their importance for plant survival or mortality under environmental stress (Choat et al., 2012; Mitchell et al., 2013). Hydraulic conductance and hydraulic vulnerability may trade off in plant stems, supporting the so-called safety vs. efficiency hypothesis (Pockman & Sperry, 2000; Maherali et al., 2004; Wheeler et al.,

2005; Hacke & Sperry, 2006; Jacobsen et al., 2007; Gleason et al., 2016). However, such relationships are less well defined in leaves, despite a growing recognition of the relative importance of leaf venation and extra-xylary compartments in regulating transpiration fluxes (Cochard et al., 2004; Buckley et al., 2015). It is generally accepted that leaf hydraulics and photosynthetic capacity are closely coupled (Scoffoni et al., 2016a), although it has been suggested that some aspects of gas exchange and hydraulic function may be decoupled by carbon-concentrating mechanisms and pulse-driven physiological strategies (Blackman et al., 2010; Ocheltree et al., 2016). Despite their importance in natural vegetation and in agriculture, reports of leaf economic and hydraulic properties in radiations of herbaceous plants are still surprisingly scarce (Dunbar-Co et al., 2009; Muir et al., 2014; Mason & Donovan, 2015b; Nolf et al., 2016). The bromeliads have attracted some recent attention from plant hydraulic researchers (e.g. North et al., 2013, 2015), but offer an excellent general opportunity to study the coordination of leaf economic and hydraulic traits in an ecophysiologically diverse herbaceous clade displaying a broad range of water-use strategies (Males, 2016).

In this investigation, we studied variation and coordination in a range of anatomical and physiological leaf traits in 50 bromeliad species representing each of the major functional types. We quantified core leaf economic traits and additional hydraulic traits in order to determine the degree of integration across various aspects of leaf physiology, the consequences for the differentiation of functional types, and to test the validity of key physiological hypotheses in the context of this important plant radiation. In particular, we aimed to test whether the evolution of external and internal water-storage systems (tank vs. leaf-succulence) have provided contrasting routes to drought avoidance in terrestrial and epiphytic bromeliads, and if succulence has weakened the coupling of LMA with other leaf economic traits due to its association with specialised non-photosynthetic hydrenchyma (Grubb et al., 2015).

Materials and Methods

Plant material and growth conditions

Fifty bromeliad species were selected to represent the ecological and phylogenetic diversity of the family. The species set included 10 C_3 terrestrials, 14 C_3 tank-epiphytes, 7 CAM terrestrials, 10 CAM tank-epiphytes, and 9 CAM atmospheric epiphytes. A full list of species with ecological notes and phylogenetic placement is provided in Supporting Information Table S1.

Plants were grown at Cambridge University Botanic Garden, UK (52.1938° N, 0.1279° E). Species from the humid tropics were grown in a tropical glasshouse with daytime temperatures of 25-30°C, night-time temperatures of 18-24°C, and relative humidity of approximately 80%. Temperate species were grown in a cool temperate house with daytime temperatures of 10-25°C, night-time temperatures above 0°C, and relative humidity of approximately 60%. All plants received a daytime photosynthetic photon flux density of at least 300 µmol m^{-2} s^{-1} through a combination of natural and artificial illumination.

As a diagnostic screen for CAM, $\delta^{13}C$ was quantified from 1 mg of dried, powdered material sampled from the centre of leaf blades and leaf tissue, using a Thermo Finnigan MAT 253 mass spectrometer (Thermo Scientific, Waltham, Massachusetts, USA) fitted with a Costech elemental analyser (Costech Analytical Technologies, Valencia, California, USA) at the Godwin Laboratory, Department of Earth Sciences, University of Cambridge. Values of $\delta^{13}C$ were similar to existing reports for most species (Crayn et al., 2015; see Supporting Information Table S2 for values), however, they suggested that all of the *Puya* Molina species (*n* = 5) were primarily performing C_3 photosynthesis under well-watered conditions.

As a rough approximation of each species' environmental niche, its location in the climate space defined by mean annual temperature (MAT, °C) and mean annual precipitation (MAP, mm) was determined. This was achieved by downloading from the Global Biodiversity Information Facility (GBIF) distributional data for each of the 48 species for which data were available, subjecting data to manual quality control (i.e. removing obvious geographic outliers or entries with problematic metadata), and then using them to interrogate the global Bioclim datasets (Hijmans et al., 2005) for the value of MAT and MAP at each retained presence point. Finally, the mean value of MAT and MAP for each species was then calculated.

Anatomical parameters

[FIGURE 2]

Examples of leaf anatomical variation among species used in this investigation are depicted in Fig. 2, which highlights key anatomical traits characterised in this study. In the bromeliads, absorptive trichomes may occur on either epidermis (or both), and differ strongly in density and absorptive capacity between functional types (Benzing, 2000). Vascular bundles occur in a single plane and alternate with longitudinal air lacunae, which may be continuous with substomatal cavities (Tomlinson, 1969). The photosynthetic mesophyll is differentiated into spongy and palisade layers in

some bromeliads adapted to high-light conditions, and in the species set used here the palisade layer was well-developed only in the CAM tank-epiphyte *Aechmea nudicaulis* (L.) Griseb. The adaxial water-storage tissue varies widely in thickness and cell dimensions. All species used in this investigation were hypostomatous, with the exception of *Catopsis berteroniana* (Schult. & Schult.f.) Mez. We focussed on vein-epidermis distance (VED) and interveinal distance, due to their relationships with leaf hydraulic capacity and extra-xylary hydraulic path-length, respectively. At least ten replicate leaves were sampled from each of five individuals, and transverse sections were hand-cut from the central portion of leaf blades and viewed under a light microscope to quantify these parameters. For the amphistomatous *C. berteroniana*, VED was strongly correlated between adaxial and abaxial surfaces (data not shown; $r^2 = 0.82$, $p = 0.512$). Stomatal density (SD) was measured by microscopic imaging of epidermal impressions of the central portion of the leaf blade microscope. Stomata were then counted on an area-normalised basis using ImageJ (NIH, Bethesda, MD, USA). Twenty replicate leaves drawn from at least five plants per species were used for all anatomical measurements.

Leaf mass per unit area

Discs were bored from four locations along the leaf axis, and dried to constant mass. Leaf mass per unit area (LMA) was calculated as the mean value of dry disc mass/disc area (g m^{-2}) across all discs per species, using four replicate sets of discs taken from five individuals per species. In no species was there was any significant variation in LMA among leaf discs sampled from the same individual (data not shown).

Intercellular air space

The intercellular air space fraction (IAS) was quantified using the vacuum infiltration technique (Unger, 1854; Smith & Heuer, 1981). A PMS pressure chamber (PMS, Albany, Oregon, USA) was used to measure native leaf water potential (Ψ_{leaf}) in leaves cut from plants at the beginning of the light period. The plants had been well watered and Ψ_{leaf} was very low in all cases (> - 0.1 MPa). Leaves were cut into 3 mm transverse slices, weighed and transferred into a beaker of isotonic mannitol solution. The beaker was placed inside a vacuum chamber, which was evacuated until the solution was almost boiling. The leaf slices were removed and blotted dry before reweighing. This process was repeated until constant weight of infiltrated samples was achieved (typically three repeats). IAS was calculated as the change in sample mass following infiltration divided by the final post-

infiltration mass and expressed as a percentage. Twenty replicate measurements were made using leaves from at least five individuals per species.

Gas exchange

All gas exchange measurements were performed on at least ten leaves drawn from at least five plants per species. The maximum rate of photosynthetic assimilation (A_{max}) at ambient CO_2 (~400 ppm) and maximum stomatal conductance (g_{smax}) were measured by gas exchange using a Li-6400XT portable photosynthesis system (Li-Cor, Lincoln, Nebraska, USA). Leaves of well-watered plants (Ψ_{leaf} > -0.1 MPa) were maintained with a constant leaf temperature (22°C) and relative humidity (85%), and a saturating PAR level determined from preliminary light-curves (usually ~300 µmol m^{-2} s^{-1}). Leaves equilibrated for at least 20 min before four data points were logged at 15 s intervals and parameters averaged. For CAM species, measurements were made in darkness during the peak assimilation period of Phase I. The instantaneous water use efficiency (iWUE) was calculated as the quotient of A_{max} and g_{smax}.

For C_3 species, measurements of dark respiration (R_D) were performed by allowing the leaf to acclimatise to darkness in the chamber for 3 min (to avoid the post-illumination respiratory burst) before four points were logged at 15 s intervals and averaged. Respiration in the light (R_L) was calculated from coupled gas exchange and fluorescence measurements (Bellasio et al. 2016), using a Li-Cor fluorometer chamber. For CAM species, R_D measurements were made in the same manner during Phase IV (direct RuBisCO-mediated CO_2 fixation through open stomata in late afternoon) where possible. In species not displaying Phase IV fixation, R_D was measured at the end of the dark period when the mesophyll acid pool was full (Wagner & Larcher, 1981). For CAM species displaying Phase IV fixation, R_L was measured using the same method as for the C_3 species. For other species, R_L was measured by cutting slices of light-acclimated leaves to allow respiratory CO_2 to escape from air spaces, and placing these in the Li-Cor chamber. Although this destructive method had the potential to introduce substantial wound-induced artefacts, the values measured were comparable to those obtained for other species using different methods, and were therefore retained for analysis.

The leaf water potential at 50% stomatal closure (P_{50S}) was obtained by measuring gas exchange and Ψ_{leaf} during gradual plant dehydration (over a period of up to 2 months for the most drought resistant species). P_{50S} was identified by using non-linear curve-fitting to predict the value of Ψ_{leaf} by which g_s had declined by 50% relative to the value measured at g_{smax} in fully hydrated plants.

Carbon, nitrogen and phosphorus assays

Carbon-to-nitrogen ratio (C:N) and leaf nitrogen content (N_{leaf}) were determined alongside $\delta^{13}C$ (see above). Photosynthetic nitrogen-use efficiency (PNUE) was calculated as the quotient of mass-normalised A_{max} and N_{leaf}. Leaf phosphorus content (P_{leaf}) was determined by sulphuric acid digestion and spectrophotometric assay (Buyarski et al. 2013).

Pressure-volume curves

Leaves were cut and immersed in water until full hydration (determined by constant mass). Rehydration times varied between 12 h and 2 d. Images of fresh leaves were used for leaf area measurement using ImageJ (US NIH, Bethesda, Maryland, USA). Hydrated leaves were gently wiped dry and allowed to reach equilibrium in a plastic bag before a Ψ_{leaf} was measured using a pressure chamber. Leaves were immediately weighed and then air dried. At regular, species-dependent intervals, coupled measurements of Ψ_{leaf} and leaf mass were made. After the final measurements, leaves were oven dried to constant dry mass. The resulting values of Ψ_{leaf} and leaf masses were analysed using the pressure-volume curve spreadsheet developed by Sack et al. (2011). Estimates of the leaf water potential at turgor loss point (Ψ_{tlp}), the bulk modulus of elasticity (ε), and area-specific capacitance (C_{FT}) were averaged across six replicate PV curves per species.

Leaf hydraulic conductance

Leaf hydraulic conductance (K_{leaf}) was measured using the evaporative flux method (Sack and Scoffoni, 2012). Leaves were cut and allowed to reach full hydration in water before being re-cut underwater and connected to the evaporative flux apparatus. 15 mM KCl in degassed reverse-osmosis water was supplied in the reservoir. The leaf was carefully inserted in a custom-built glass cuvette fitted with fans to minimise boundary layer resistance. A water jacket coupled to a water bath was used to control cuvette air temperature, and humidified air was fed into the chamber to achieve a specific dew point. Leaf temperature was maintained at 25°C throughout, and relative humidity was maintained at 85% by varying the dew point. The system was illuminated by a halogen lamp to provide 300 µmol m^{-2} s^{-1} at leaf-level for C_3 species, while measurements on CAM species were performed during the night in darkness. Leaves were allowed to transpire under constant conditions for at least 30 min. The leaf was then removed from the system and placed in a plastic bag to equilibrate before the measurement of final Ψ_{leaf} using a pressure chamber. Leaf area was

measured using ImageJ. Area-specific K_{leaf} (mmol m^{-2} s^{-1} MPa^{-1}) was calculated as the molar quantity of water drawn from the balance reservoir (mmol) divided by the product of leaf area (m^2), duration (s) and the driving force (MPa). Since all measurements were made at the same leaf temperature, no standardisation was performed to control for differences in viscosity.

Leaf hydraulic vulnerability curves

Hydraulic vulnerability curves were constructed by measuring K_{leaf} (see above) at intervals of Ψ_{leaf}. Preliminary comparison was made of vulnerability curves constructed using the standard bench-drying methodology and using overpressure. In the former, initially fully-hydrated leaves were allowed to dry on the bench between regular measurements of K_{leaf}. In the latter, leaves were dehydrated by very gradually applied overpressure in the pressure chamber. Leaves were pressurised until the extrusion of solution from the cut end of the xylem ceased, and K_{leaf} was then measured. This was performed at evenly-spaced pressure increments, using separate five replicate leaves from different plants for measurements at each interval. Comparison of the overpressure and bench-drying methodologies showed that in these bromeliad species they produced equivalent results, despite the many artefacts that could be introduced by damage to tissue structure in the overpressure method (comparative data are shown in Supporting Information File S1). The overpressure method was considerably faster than bench drying (hours rather than days or weeks, depending on the species), and was therefore used for subsequent repeat measurements for all species. P_{50L} was determined as the value of Ψ_{leaf} on a sigmoidal curve fitted to the data where K_{leaf} had declined to 50% of its maximum value in fully hydrated leaves ($K_{leafmax}$).

Statistical analysis

All statistical analyses were performed using R (R Development Core Team, 2008). Linear or non-linear regression was used on a pairwise basis to identify trait relationships, and analysis of variance (ANOVA) was used to identify differences in trait values between functional types. In general, r^2 values > 0.25 were interpreted as suggesting a mechanistic relationship between traits (Poorter et al., 2014). It was not possible to perform phylogenetic analysis of trait data due to the current lack of resolution in the phylogeny of Bromeliaceae. Principal components analysis (PCA) was performed in R to identify major axes of variation in the total dataset of functional traits.

Results

[FIGURE 3]

The bromeliads occur in a wide variety of biomes, habitats and microhabitats throughout the Neotropics and into adjacent temperate zones in both hemispheres. This diversity in environmental niches is mirrored by the relatively large area of environmental and leaf economic trait-space occupied by the representative bromeliad species used in this investigation (Fig. 3a,b). The full results for all species are available in Supporting Information Table S2. Values for many physiological rates were an order of magnitude lower relative to many other angiosperm groups, including for A_{max} (0.70-6.81 µmol m^{-2} s^{-1}), g_{smax} (0.005-0.243 mol m^{-2} s^{-1}), $K_{leafmax}$ (0.01-5.84 mmol m^{-2} s^{-1} MPa^{-1}) R_L (0.18-0.46 µmol m^{-2} s^{-1}), and R_D (0.25-0.71 µmol m^{-2} s^{-1}), and values of N_{leaf} (0.45-1.71%) and P_{leaf} (0.002-0.024%) were also low. There was considerable variation in IAS (3.88-19.42%), iWUE (15.2-328.0 µmol mol^{-1}), LMA (38.3-380.0 g m^{-2}), and PNUE (0.26-11.11). All values of Ψ_{tlp} (-1.57 - -0.63 MPa) and P_{50L} (-1.74 - -0.60 MPa) were rather high, suggesting that bromeliads are relatively drought-sensitive at the cellular level. C_{FT} was high (2.38-14.05 mol m^{-2} MPa^{-1}), particularly among species with thick adaxial layers of water-storage tissue. ε occasionally reached extremely low values (1.60-21.91 MPa). Interveinal distances (IVD) were comparable towards their lower limit to C_3 grasses (190.0-426.7 µm; Griffiths et al., 2013), while vein-epidermis distance (VED) was highly variable (90.0-495.0 µm). Stomatal responses to Ψ_{leaf} were quantified as P_{50S} (Fig. 4), which was not correlated with other leaf traits and consistently less negative than P_{50L}, ranging from -0.62 to -0.27 MPa. Examples of leaf hydraulic vulnerability curves and g_s- Ψ_{leaf} curves used to derive P_{50L} and P_{50S} are shown in Fig. 5.

[FIGURE 4]

[FIGURE 5]

Coordinated variation in bromeliad leaf traits

[FIGURE 6]

Pairwise regression analysis of all continuous variables yielded correlations that supported most of the core relationships of leaf economic theory. Key relationships and underlying data are displayed in Fig. 6, with the statistically significant correlations being detailed in Table 1. The full trait dataset is also available in tabulated form in Supporting Information Table S2.

[TABLE 1]

Species-specific absolute values of K_{leaf} and g_s at $\Psi_{leaf} = P_{50S}$ and $\Psi_{leaf} = P_{50L}$ predicted by curve-fitting were compared. When values were log-transformed, there was a statistically significant positive relationship between g_s and K_{leaf} at P_{50S} ($r^2 = 0.85$, $p < 0.001$; Fig. 7a) and at P_{50L} ($r^2 = 0.60$, $p < 0.001$; Fig. 7b), with the highest values occurring among C_3 terrestrials, followed by C_3 tank-epiphytes. Those species able to maintain higher absolute K_{leaf} at more negative Ψ_{leaf} could therefore support higher absolute g_s. Furthermore, a robust positive correlation between log-transformed values of P_{50L} and the absolute value of K_{leaf} at P_{50L} ($r^2 = 0.42$, $p < 0.001$; Fig. 7c) suggests that species that are more resistant to dehydration maintain higher absolute as well as proportional hydraulic conductance at more negative Ψ_{leaf} than less resistant species. Furthermore, across all species, there was a strong negative relationship between $K_{leafmax}$ and P_{50L} ($r^2 = 0.52$, $p < 0.001$; Fig. 7d), apparently contradicting the hydraulic safety-efficiency hypothesis.

[FIGURE 7]

A_{max} and $K_{leafmax}$ were decoupled in CAM atmospheric epiphytes ($r^2 = -0.13$, $p = 0.799$), and A_{max}, g_{smax} and IAS were decoupled in all CAM functional types ($p > 0.05$ for all pairwise relationships). Interestingly, $K_{leafmax}$ was not correlated with IVD ($r^2 = -0.02$, $p = 0.693$), perhaps implying that interspecific differences are related to xylem structural properties we did not measure, or that extra-xylary factors are more important in determining overall leaf hydraulic conductance. The strong positive correlation between P_{50L} and Ψ_{tlp} ($r^2 = 0.93$, $p < 0.001$) is suggestive of the importance of extra-xylary vulnerability to embolism, or at least of strong concerted evolution of these traits. Meanwhile C_{FT} and ε were negatively correlated ($r^2 = 0.29$, $p < 0.001$), suggestive of the importance of cell wall flexibility for the recharge of succulent tissues.

Principal components analysis

Log-transformed data for all continuous variables were used to perform principal component analyses (PCA) including data for all species. Full results are available in Supporting Information Table S3. For the core leaf economic traits, loadings displayed approximately the expected directionality (Fig. 8a). The first two principal components explained 48.3% and 18.7% of the variance respectively. The eigenvectors of traits related to vascular geometry, tissue density and water storage showed strong alignment, while a second, looser grouping of trait eigenvectors included most gas exchange, hydraulic and nutrient-related traits. The presence of these two axes implies a certain degree of independence in variation in structural and functional traits. The eigenvector for P_{50S} did not align with that of any other trait. Functional types segregated quite

clearly in the morphospace defined by the first two principal components (Fig. 8b), showing that there is a clear physiological and anatomical basis for the differentiation of ecophysiological functional types in the Bromeliaceae. C_3 terrestrials clustered towards the high-productivity end of the axis incorporating traits related to physiological function, while C_3 tank-epiphytes were distinctively positioned towards the end of the structural axis of variation defined by low tissue density and high PNUE. C_3 functional types tended to show greater variation along the axis associated with leaf structure, whereas the CAM functional types varied primarily along the axis associated with physiological functions.

[FIGURE 8]

Comparison of trait values between functional types

Insights were obtained by considering the differences in trait values between C_3 terrestrials, C_3 and CAM tank-epiphytes, and CAM atmospheric epiphytes. Comparisons were performed by analysis of variance according to an evolutionary scheme in which CAM terrestrials and C_3 tank-epiphytes arose from C_3 terrestrials, CAM tank-epiphytes from CAM terrestrials, C_3 tank-epiphytes from C_3 terrestrials, and CAM atmospheric epiphytes from C_3 tank-epiphytes. Mean values of traits for each functional type are shown in Table 2, and complete data for all species are available in Supporting Information Table S2.

[TABLE 2]

Relative to C_3 terrestrials, CAM terrestrials showed significantly lower A_{max} ($F = 45.40$, $p < 0.001$), g_{smax} ($F = 48.30$, $p < 0.001$), $K_{leafmax}$ ($F = 40.12$, $p < 0.001$), SD ($F = 5.14$, $p = 0.039$), R_L ($F = 78.35$, $p < 0.001$), R_D ($F = 215.50$, $p < 0.001$), N_{leaf} ($F = 6.08$, $p = 0.026$), P_{leaf} ($F = 52.80$, $p < 0.001$), PNUE ($F = 5.37$, $p = 0.035$), ε ($F = 30.01$, $p < 0.001$), less negative P_{50L} ($F = 26.23$, $p < 0.001$), Ψ_{tlp} ($F = 40.81$, $p < 0.001$), and higher C:N ($F = 7.57$, $p = 0.015$), iWUE ($F = 8.37$, $p = 0.011$), and VED ($F = 6.95$, $p = 0.019$). These differences are generally reflective of slower-growth strategies and more conservative water use, consistent with the bioclimatic relations of C_3 and CAM bromeliads.

C_3 tank-epiphytism, relative to the C_3 terrestrial habit, was associated with reduced A_{max} ($F = 5.05$, $p = 0.016$), g_{smax} ($F = 9.59$, $p = 0.001$), $K_{leafmax}$ ($F = 29.52$, $p < 0.001$), SD ($F = 4.88$, $p = 0.018$), R_L ($F = 40.49$, $p < 0.001$), and R_D ($F = 41.26$, $p < 0.001$). C_3 tank-epiphytes also showed significantly lower C_{FT} ($F = 5.88$, $p = 0.009$), suggesting that investment in external capacitance (the tank) reduces the requirement for internal capacitance (in succulent water-storage tissue). However, less negative values of P_{50L} ($F = 47.07$, $p < 0.001$), P_{50S} ($F = 18.70$, $p < 0.001$) and Ψ_{tlp} ($F = 44.82$, $p < 0.001$) also

348 occur in C_3 tank-epiphytes. Lower LMA (F = 17.99, p < 0.001), P_{leaf} (F = 48.58, p < 0.001) and VED (F =
349 8.96, p = 0.001) in C_3 tank-epiphytes may reflect adaptation to resource limitation and maximisation
350 of canopy area under these conditions. Higher IAS (F = 3.94, p = 0.035) could also reduce
351 construction costs, as well as providing ventilation to submerged tissues.

352 CAM tank-epiphytes in the Bromelioideae subfamily showed similar differences from terrestrial CAM
353 species, including reduced C_{FT} (F = 27.20, p < 0.001), g_{smax} (F = 10.94, p = 0.005), LMA (F = 27.16, p <
354 0.001), and increased IAS (F = 8.92, p = 0.010) and PNUE (F = 5.82, p = 0.030). However, they
355 displayed higher $K_{leafmax}$ (F = 14.12, p = 0.002), SD (F = 5.60, p = 0.033) and iWUE (F = 9.18, p = 0.009)
356 than their terrestrial counterparts, suggesting that the combination of tank and absorptive
357 trichomes may facilitate enhanced productivity. Unlike in the case of the C_3 lineages, IVD, P_{leaf}, P_{50L},
358 P_{50S}, R_D, R_L and Ψ_{tlp} did not differ significantly between CAM terrestrials and CAM tank-epiphytes (p >
359 0.05). This reflects the fact that terrestrial CAM species already engage in highly conservative water-
360 use strategies, which may have made the epiphytic habit easier to evolve.

361 Relative to the C_3 tank-epiphytes of the Tillandsioideae from which they evolved, CAM atmospheric
362 epiphytes showed significantly lower A_{max} (F = 146.80, p < 0.001), $K_{leafmax}$ (F = 61.84, p < 0.001), g_{smax} (F
363 = 78.78, p < 0.001), SD (F = 69.35, p < 0.001) and iWUE (F = 82.21, p < 0.001). These reductions, in
364 combination with lower R_L (F = 5.08, p = 0.035) and R_D (F = 14.30, p = 0.001), are associated with
365 lower productivity compared with C_3 tank-epiphytes. Less negative Ψ_{tlp} (F = 8.15, p = 0.009)
366 corresponds to an increased investment in drought resistance over drought tolerance. In terms of
367 leaf structure, lower IAS (F = 40.92, p < 0.001) and higher C_{FT} (F = 47.09, p < 0.001) in atmospheric
368 epiphytes are the result of dense tissue packing. Reduced N_{leaf} (F = 5.16, p = 0.033) and P_{leaf} (F =
369 46.88, p < 0.001) might reflect the adaptation of atmospheric epiphytes to low mineral nutrient
370 supply.

371

372 **Discussion**

373 The Bromeliaceae is an important emerging model family in plant evolutionary ecology and
374 physiology (Males, 2016; Palma-Silva et al., 2016). The evolution of ecological diversity in the
375 bromeliads is a complex story, involving multiple nested radiations, some spurred by key innovations
376 that have facilitated enhanced diversification rates (Givnish et al., 2014; Silvestro et al., 2014). Major
377 physiographic processes on the South American continent have also likely made important
378 contributions to the evolutionary history of the bromeliads by determining the diversity and extent
379 of niche space available for colonisation. The classic example is the pulsed uplift of the Andean
380 cordillera (Gentry, 1982), but the legacy of periodic marine incursions into the Amazon basin and

dynamic changes in forest composition and extent is probably also imprinted on the biogeography and diversity of many Neotropical plant lineages (Rull, 2011). The potential for the investigation of links between physiographic change and evolutionary dynamics is limited by a very sparse fossil record (Benzing, 2000), and while extensive consideration has previously been given to the relationships between key innovations, functional types and species diversification (Givnish et al., 2014; Silvestro et al., 2014), the interactions between trait-network architecture and functional type differentiation have remained little explored. This is despite the fact that relevant leaf trait values are rapidly quantifiable, and that trait variation has presumably been important in promoting ecological divergences both within and between functional types. Our data provide crucial insights into the nature of trait divergences between functional types, and place variation among bromeliad species into a wider context by positioning them on the leaf economic spectrum. They also shed light on critical outstanding questions in leaf hydraulics, and represent a significant contribution towards ameliorating the underrepresentation of herbaceous species in trait-based ecophysiology.

Functional trait divergence and ecological diversity in the bromeliads

The ecological differentiation of bromeliads into distinctive functional types was critical to their successful radiation into numerous highly stressful habitats, including deserts, salt crusts, seasonal riverbeds, cliff-faces, alpine tundra and forest canopies (Benzing, 2000). Until now, the variation in functional traits underpinning this differentiation had never been systematically investigated. Our analysis demonstrates that the ecological divergence of functional types has a clear basis in anatomical and physiological trait change and trait-network rewiring (Fig. 9). Functional types segregated in the multivariate trait space almost completely, suggesting that differences in a limited number of traits can account for a large proportion of the ecophysiological distinctiveness of each functional type.

[FIGURE 9]

The most basic condition in the Bromeliaceae is the combination of the C_3 photosynthetic pathway with the terrestrial habit. Although many species of this type are adapted to low-exposure, mesic habitats, others occupy more stressful environments, including Andean tundra and deciduous seasonally-dry tropical forests. Much of this specialisation can be attributed to variety in leaf form (Males, in review), which was particularly marked in this functional type. CAM has evolved convergently in multiple lineages of terrestrial bromeliads that occur principally in semi-arid, coastal or high-altitude environments, suggesting a consistent physiological advantage of CAM under water-

limited conditions (cf. Griffiths & Smith, 1983). In our dataset, clear functional trait differences between C_3 and CAM terrestrial species suggest that CAM can act as a downward gear-change in physiological productivity. This may nevertheless provide a competitive advantage in highly stressful environments, as illustrated by the radiations of CAM terrestrial bromeliad lineages such as *Hechtia* Klotzsch and the xeric clade of the Pitcairnioideae (*Deuterocohnia* Mez, *Dyckia* Schult.f. and *Encholirium* Schult. & Schult.f.).

The parallel origins of tank-epiphytism in the CAM Bromelioideae lineage and C_3 Tillandsioideae lineage were transformative events both in the evolutionary history of the Bromeliaceae and for the ecology of the Neotropics. Reduced interspecific competition and enhanced light availability are two factors that may have benefited the pioneering epiphytic lineages and allowed them to undergo explosive diversification (Givnish et al., 2014). Relative to terrestrial species, tank-epiphytes of either photosynthetic pathway display improved PNUE and reduced leaf construction costs through well-developed aerenchyma and relaxed selection for internal capacitance. These differences are all of obvious utility in meeting the unique challenges of the epiphytic habit. Since fewer traits differed between CAM terrestrials and CAM tank-epiphytes than between C_3 terrestrials and C_3 tank-epiphytes, the pre-existence of CAM in the progenitor lineage of the tank-epiphyte Bromelioideae may have facilitated survival in water-limited arboreal environments during the early stages of the evolutionary transition (Zotz & Hietz, 2001; Crayn et al., 2004; Givnish et al., 2014; Silvestro et al., 2014). CAM tank-epiphytes also do not appear to differ as strongly from CAM terrestrials in terms of bioclimatic envelope as do C_3 tank-epiphytes from C_3 terrestrials, but the considerable and confounding importance of microenvironmental factors means that further careful work will be required to elucidate the detailed relationships between the leaf traits and bioclimatic distributions of bromeliad species of different functional types. Moreover, much better phylogenetic resolution based on denser taxon sampling will be required before detailed hypotheses about trait trajectories during the evolution of specific lineages can be tested.

The atmospheric epiphytes of the genus *Tillandsia* L. represent one of the most striking examples of a vascular plant radiation in the Neotropics. The habitats and outer-canopy microhabitats they occupy are often particularly water-limited, such that their success has been contingent upon three innovations: CAM, highly-effective and abundant absorptive foliar trichomes, and morphological reduction through neoteny. Since these species represent the ultimate expression of extreme epiphytism, alongside the shootless orchids (Benzing & Ott, 1981), it is not surprising that they show very low physiological activity both on an absolute basis and relative to the C_3 tank-epiphytes from which they evolved. Despite previous suggestions that the dense indumentum of absorptive foliar trichomes in these species should negate the need for axial water transport through veins (Benzing,

2000), our data demonstrate the potential for vascular water distribution at low fluxes. Further experiments will be needed to compare the relative importance of vascular and trichome-/aquaporin-mediated water distribution (cf. Ohrui et al., 2007).

A central theme that emerges from our analysis is the association of functional type differentiation with modification of trait-network constraints. The decoupling and recoupling of variation in leaf economic and hydraulic traits has provided exceptional flexibility for trait evolution and combination in the Bromeliaceae, and the mechanistic basis of these events should therefore be a priority for further investigation. Indeed, the process of innovation-driven trait-network rewiring may prove to be of more general importance when similar treatments of other important nested radiations are carried out. We expect it to be particularly clear across evolutionary transitions in photosynthetic pathway, which are typically associated with structural differentiation of the leaf alongside changes in biochemistry and physiological efficiency and rhythms. Another example, illustrated by our data, is succulence. Consistent with observations in Mediterranean plant communities made by Grubb et al. (2015, leaf economic relationships were weaker in more succulent bromeliad groups (i.e. CAM terrestrials and CAM atmospheric epiphytes). All else being equal, the construction of specialised adaxial water-storage tissue will involve an increase in LMA, but need not affect photosynthetic capacity as the biochemical capacity and CO_2 conductance of the photosynthetic chlorenchyma tissue can remain unchanged. Ripley et al. (2013) have recently demonstrated how this leads to a decoupling of the degree of succulence and gas exchange in the Aizoaceae.

Leaf hydraulic trait interactions in the bromeliads

Strong correlations between A_{max} and $K_{leafmax}$ across all species suggest that leaf gas exchange and hydraulic conductance have evolved in a coordinated manner in the bromeliads. This is consistent with a growing corpus of data covering many, primarily woody, plant groups (Brodribb et al., 2002, 2005, 2007; Scoffoni et al., 2016a). The negative relationship between $K_{leafmax}$ and P_{50L} in the bromeliads does not support the hydraulic safety vs. efficiency hypothesis. Blackman et al. (2010) had suggested that the likelihood of finding evidence for this hypothesis in leaves was low because P_{50L} and $K_{leafmax}$ should relate to different aspects of leaf anatomy. Specifically, these authors expected P_{50L} to correlate with xylem conduit structure, and $K_{leafmax}$ to be determined by venation density, mesophyll architecture, and aquaporin regulation. Scoffoni et al. (2016b) have recently demonstrated that xylem structure is an important determinant of leaf hydraulic vulnerability in other angiosperms. While this may also be true for the bromeliads, our data are consistent with the possibility that both $K_{leafmax}$ and P_{50L} are strongly influenced by extra-xylary factors. The strong

correlation between Ψ_{tlp} and P_{50L} across all species is in accord with reports from other plant groups (Blackman et al., 2010; Scoffoni et al., 2011, 2012; Villagra et al., 2013; Nardini & Luglio, 2014), and the fact that P_{50L} approximately equals Ψ_{tlp} could support the contention that hydraulic resistance and vulnerability resides predominantly in the extra-xylary compartment (Cochard et al., 2004; Blackman et al., 2010; Scoffoni et al., 2014). Loss of turgor in mesophyll cells can cause changes in the conformation or continuity of transcellular and apoplastic pathways of extra-xylary water transport, impacting on the dynamics of leaf hydraulic properties during dehydration (Scoffoni et al., 2017). P_{50L} was also negatively correlated with ε in C_3 species, consistent with the idea that inflexible cell walls confer improved drought resistance because they facilitate large changes in water potential in response to small changes in relative water content (Niinemets, 2001; Blackman et al, 2010). The role of aquaporins in variable leaf hydraulic conductance in the bromeliads is unknown, but warrants further study (cf. Shatil-Cohen et al., 2011; Prado et al., 2013; Sade et al., 2014). Following the observation that IVD was apparently not related to $K_{leafmax}$, more detailed investigation of the functional significance of variation in bromeliad vascular properties is currently underway.

Stomatal density is an important predictor of hydraulic and photosynthetic capacity across the bromeliads, but the independence of variation in P_{50S} from variation in all other traits, considered alongside the fact that P_{50S} was consistently and substantially less negative than P_{50L}, is intriguing. It implies that the stomatal behaviour of bromeliads has evolved along a unique trajectory and yet is critical to the control of leaf water balance. Stomatal morphology is highly diverse within the Bromeliaceae (Tomlinson, 1969). Following some early reports on stomatal sensitivity to humidity in the bromeliads (Lange & Medina, 1979; Adams & Martin, 1986), recent work has aimed to determine how differences in stomatal morphology might translate to differences in stomatal kinetics in response to endogenous and exogenous stimuli, and relate to the ecological differentiation of functional types (Males & Griffiths, in review).

The role of capacitance in vascular plant leaf hydraulics is increasingly well-studied. Understanding how water is moved into storage and subsequently metered out to sustain transpiration under limited soil water availability is both an interesting question in evolutionary physiology (Blackman & Brodribb, 2011; Griffiths, 2013), and critical in applied contexts such as the improvement of crop drought resistance. In the bromeliads, the negative relationship between C_{FT} and A_{max} and positive relationship between C_{FT} and LMA show that more succulent species tend to be situated at the slower-growing end of the leaf economic spectrum. However, C_3 terrestrial succulents (particularly *Puya* spp.) supported relatively high photosynthetic capacity, perhaps allowing them to make considerable carbon gains during pulses of water availability before reducing gas exchange rates and relying on stored water during drought periods. Nevertheless, the negative relationship between C_{FT}

514 and A_{max} in CAM bromeliads suggests that there may be a trade-off between degree of succulence
515 and photosynthetic capacity, perhaps due to diffusion constraints (Maxwell et al., 1997). Certain
516 succulent dicot lineages have evolved 'three-dimensional' venation that has released the constraints
517 on succulence imposed by the presence of a single vascular plane (Ogburn & Edwards, 2013), but
518 this innovation has not arisen in the Bromeliaceae. Future research might seek to explore the
519 interactions between selection for enhanced efficiency of recharge of water-storage tissue and
520 optimal water-use efficiency and how these have affected trait evolution under different water-
521 availability regimes (Males, 2017).

522 In summary, trait variation in the highly diverse Bromeliaceae can be accommodated in the existing
523 framework of the leaf economic spectrum, with allowances made for trait-network rewiring
524 associated with functional type differentiation driven by innovations such as CAM, tank-epiphytism
525 and neoteny. Trait-level adaptation to contrasting habits and growth-strategies is reflected by the
526 clear segregation of functional types in a multivariate space defined by key anatomical and
527 physiological traits. Our data are also consistent with the hypothesis leaf hydraulics and gas
528 exchange are coupled across the bromeliads, but the hydraulic safety vs. efficiency trade-off is not
529 apparent, and hydraulic sensitivity to declining leaf water potential may reside primarily at the
530 stomatal and extra-xylary levels. Future work should attempt to explore in more detail the specific
531 structure-function relationships integral to ecophysiological differentiation in the bromeliads, as well
532 as beginning to explore the molecular basis of trait variation. As phylogenetic resolution continues to
533 improve, exciting opportunities will also emerge to test complex evolutionary hypotheses in an
534 explicit and structured manner.

535

536 **Acknowledgements**

537 We are grateful to Brent Helliker for assistance in preparing equipment for hydraulic measurements,
538 and to Jessica Royles and two anonymous reviewers for helpful comments on an earlier version of
539 the manuscript.

540

541 **Conflict of Interest Statement**

542 The authors declare no conflict of interest.

543

544

References

Adams, W.W. & Martin, C.E. (1986) Physiological consequences of changes in life form of the Mexican epiphyte *Tillandsia deppeana* (Bromeliaceae). *Oecologia* 70, 298-304.

Beaulieu, J.M., Leitch, I.J. & Knight, C.A. (2007) Genome size evolution in relation to leaf strategy and metabolic rates revisited. *Annals of Botany* 99, 495-505.

Bellasio, C., Beerling, D.J. & Griffiths, H. (2016) An Excel tool for deriving key photosynthetic parameters from combined gas exchange and chlorophyll fluorescence: theory and practice. *Plant, Cell & Environment* 39, 1180-1197.

Benzing, D.H. (2000). *Bromeliaceae: Profile of an adaptive radiation*. Cambridge, UK: Cambridge University Press.

Benzing, D.H. & Ott, D.W. (1981) Vegetative reduction in epiphytic Bromeliaceae and Orchidaceae: its origin and significance. *Biotropica* 13, 131-140.

Blackman, C.J. & Brodribb, T.J. (2011) Two measures of leaf capacitance: insights into the water transport pathway and hydraulic conductance in leaves. *Functional Plant Biology* 38, 118-126.

Blackman, C.J., Brodribb, T.J. & Jordan, G.J. (2010) Leaf hydraulic vulnerability is related to conduit dimensions and drought resistance across a diverse range of woody angiosperms. *New Phytologist* 188, 1113-1123.

Brodribb, T.J., Feild, T.S. & Jordan, G.J. (2007) Leaf maximum photosynthetic rate and venation are linked by hydraulics. *Plant Physiology* 144, 1890-1898.

Brodribb, T.J., Holbrook, N.M. & Gutiérrez, M.V. (2002) Hydraulic and photosynthetic co-ordination in seasonally dry tropical forest trees. *Plant, Cell & Environment* 25, 1435-1444.

Brodribb, T.J., Holbrook, N.M., Zwieniecki, M.A. & Palma, B. (2005) Leaf hydraulic capacity in ferns, conifers and angiosperms: impacts on photosynthetic maxima. *New Phytologist* 165, 839-846.

Brodribb, T.J., Jordan, G.J. & Carpenter, R.J. (2013) Unified changes in cell size permit coordinated leaf evolution. *New Phytologist* 199, 559-570.

Buckley, T.N., John, G.P., Scoffoni, C. & Sack, L. (2015) How does leaf anatomy influence water transport outside the xylem? *Plant Physiology* 168, 1616-1635.

Butcher, D. & Gouda, E. (2016) The new Bromeliad Taxon list. [WWW document] URL http://botu07.bio.uu.nl/bcg/taxonList.php [accessed 12 Dec 2016]

574 Buyarski, C. & Brovold, S. (2013) *Plant phosphorus protocol- sulfuric acid digestion*. [WWW
575 document] URL http://prometheuswiki.publish.csiro.au/tiki-
576 index.php?page=Plant+Phosphorus+Protocol+-+Sulfuric+acid+digestion [accessed 20 May 2015]

577 Choat, B., Jansen, S., Brodribb, T.J., Cochard, H., Delzon, S., Bhaskar, R., … & Zanne, A.E. (2012)
578 Global convergence in the vulnerability of forests to drought. *Nature* 491, 752-755.

579 Cochard, H., Nardini, A. & Coll, L. (2004) Hydraulic architecture of leaf blades: where is the main
580 resistance? *Plant, Cell & Environment* 27, 1257-1267.

581 Crayn, D.M., Winter, K., Schulte, K. & Smith, J.A.C. (2015) Photosynthetic pathways in Bromeliaceae:
582 phylogenetic and ecological significance of CAM and C_3 based on carbon isotope ratios for 1893
583 species. *Botanical Journal of the Linnean Society* 178, 169-221.

584 Crayn, D.M., Winter, K. & Smith, J.A.C. (2004) Multiple origins of crassulacean acid metabolism and
585 the epiphytic habit in the Neotropical family Bromeliaceae. *Proceedings of the National Academy of*
586 *Sciences of the USA* 101, 3703-3708.

587 Díaz, S., Kattge, J., Cornelissen, J.H.C., Wright, I.J., Lavorel, S., Dray, S., … & Gorné, L.D. (2016) The
588 global spectrum of plant form and function. *Nature* 529, 167-171.

589 Donovan, L.A., Maherali, M., Caruso, C.M., Huber, H. & de Kroon, H. (2011) The evolution of the
590 worldwide leaf economics spectrum. *Trends in Ecology & Evolution* 26, 88-95.

591 Dunbar-Co, S., Sporck, M.J. & Sack, L. (2009) Leaf trait diversification and design in seven rare taxa of
592 the Hawaiian Plantago radiation. *International Journal of Plant Sciences* 170, 61-75.

593 Gentry, A.H. (1982) Neotropical floristic diversity: phytogeographical connections between Central
594 and South America, Pleistocene climatic fluctuations, or an accident of the Andean orogeny? *Annals*
595 *of the Missouri Botanic Garden* 69, 557-593.

596 Givnish, T.J., Barfuss, M.H.J., Van Ee, B., Riina, R., Schulte, K., Horres, R., … & Sytsma, K.J. (2014)
597 Adaptive radiation, correlated and contingent evolution, and net species diversification in
598 Bromeliaceae. *Molecular Phylogenetics and Evolution* 71, 55-78.

599 Gleason, S.M., Westoby, M., Jansen, S., Choat, B., Hacke, U.G., Pratt, R.B., … & Zanne, A.E. (2016)
600 Weak tradeoff between xylem safety and xylem-specific hydraulic efficiency across the world's
601 woody plant species. *New Phytologist* 209, 123-136.

602 Griffiths, H. (2013) Plant venation: from succulence to succulents. *Current Biology* 23, R340-R341.

603 Griffiths, H. & Smith, J.A.C. (1983) Photosynthetic pathways in the Bromeliaceae of Trinidad:
604 relations between life-forms, habitat preference and the occurrence of CAM. *Oecologia* 60, 176-184.

605 Griffiths, H., Weller, G., Toy, L.F. & Dennis, R.J. (2013) You're so vein: bundle sheath physiology,
606 phylogeny and evolution in C_3 and C_4 plants. *Plant, Cell & Environment* 36, 249-261.

607 Grubb, P.J., Marañón, T., Pugnaire, F.I. & Sack, L. (2015) Relationships between specific leaf area and
608 leaf composition in succulent and non-succulent species of contrasting semi-desert communities in
609 south-eastern Spain. *Journal of Arid Environments* 9, 3-33.

610 Hacke, U., & Sperry, J. (2006) Scaling of angiosperm xylem structure with safety and efficiency. *Tree*
611 *Physiology* 26, 689-701.

612 Hijmans, R.J., Cameron, S.E., Parra, J.L., Jones, P.G. & Jarvis, A. (2005) Very high resolution
613 interpolated climate surfaces for global land areas. *International Journal of Climatology* 25, 1965-
614 1978.

615 Jacobsen, A.L., Pratt, R.B., Ewers, F.W. & Davis, S.D. (2007) Cavitation resistance among 26 chaparral
616 species of southern California. *Ecological Monographs* 77, 99-115.

617 Lange, O.L. & Medina, E. (1979) Stomata of the CAM plant *Tillandsia recurvata* respond directly to
618 humidity. *Oecologia* 40, 357-363.

619 Maherali, H, Pockman, W.T. & Jackson, R.B. (2004) Adaptive variation in the vulnerability of woody
620 plants to xylem cavitation. *Ecology* 85, 2184-2199.

621 Males, J. (2016) Think tank: water relations of Bromeliaceae in their evolutionary context. *Botanical*
622 *Journal of the Linnean Society* 181, 415-440.

623 Males, J. (2017) Secrets of succulence. *Journal of Experimental Botany* in press.

624 Mason, C.M. & Donovan, L.A. (2015a) Does investment in leaf defenses drive changes in leaf
625 economic strategy? A focus on whole-plant ontogeny. *Oecologia* 177, 1053-1066.

626 Mason, C.M. & Donovan, L.A. (2015b) Evolution of the leaf economics spectrum in herbs: evidence
627 from environmental divergences in leaf physiology across *Helianthus* (Asteraceae). *Evolution* 69,
628 2705-2720.

629 Maxwell, K., von Caemmerer, S. & Evans, J.R. (1997) Is a low internal conductance to CO_2 diffusion a
630 consequence of succulence in plants with Crassulacean acid metabolism? *Functional Plant Biology*
631 24, 777-786.

Mitchell, P.J., O'Grady, A.P., Tissue, D.T., White, D.A., Ottenschlaeger, M.L. & Pinkard, E.A. (2013) Drought response strategies define the relative contributions of hydraulic dysfunction and carbohydrate depletion during tree mortality. *New Phytologist* 197, 862-872.

Muir, C.D., Hangarter, R.P., Moyle, L.C. & Davis, P.A. (2014) Morphological and anatomical determinants of mesophyll conductance in wild relatives of tomato (*Solanum* sect. *Lycopersicon*, sect. *Lycopersicoides*; Solanaceae). *Plant, Cell & Environment* 37, 1415-1426.

Nardini, A. & Luglio, J. (2014) Leaf hydraulic capacity and drought vulnerability: possible trade-offs and correlations with climate across three major biomes. *Functional Ecology* 28, 810-818.

Niinemets, U. (2001) Global-scale climatic controls of leaf dry mass per area, density, and thickness in trees and shrubs. *Ecology* 82, 453-469.

Niinemets, U., Portsmuth, A., Tena, D., Tobias, M., Matesanz, S. & Valladares, F. (2007a) Do we underestimate the importance of leaf size in plant economics? Disproportional scaling of support costs within the spectrum of leaf physiognomy. *Annals of Botany* 100, 283-303.

Niinemets, U., Portsmuth, A. & Tobias, M. (2007b) Leaf shape and venation pattern alter the support investments within leaf lamina in temperate species: a neglected source of leaf physiological differentiation? *Functional Ecology* 21, 28-40.

Nolf, M., Rosani, A., Ganthaler, A., Beikircher, B. & Mayr, S. (2016) Herb hydraulics: inter- and intraspecific variation in three *Ranunculus* species. *Plant Physiology* 170, 2085-2094.

North, G.B., Browne, M.G., Fukui, K., Maharaj, F.D.H., Phillips, C.A. & Woodside, W.T. (2015) A tale of two plasticities: Leaf hydraulic conductances and related traits diverge for two tropical epiphytes from contrasting light environments. *Plant, Cell & Environment* 39, 1408-1419.

North, G.B., Lynch, F.H., Maharaj, F.D., Phillips, C.A. & Woodside, W.T. (2013) Leaf hydraulic conductance for a tank bromeliad: axial and radial pathways for moving and conserving water. *Frontiers in Plant Science* 4, 78.

Ocheltree, T.W., Nippert, J.B. & Prasad, P.V.V. (2016) A safety vs efficiency trade-off identified in the hydraulic pathway of grass leaves is decoupled from photosynthesis, stomatal conductance and precipitation. *New Phytologist* 210, 97-107.

Ogburn, R.M. & Edwards, E.J. (2013) Repeated origin of three-dimensional leaf venation releases constraints on the evolution of succulence in plants. *Current Biology* 23, 722-726.

661 Ohrui, T., Nobira, H., Sakata, Y., Taji, T., Yamamoto, C., Nishida, K., … & Tanaka, S. (2007) Foliar
662 trichome- and aquaporin-aided water uptake in a drought-resistant epiphyte, *Tillandsia ionantha*
663 Planchon. *Planta* 227, 47-56.

664 Palma-Silva, C., Leal, B.S.S., Chaves, C.J.N. & Fay, M.F. (2016) Advances in and perspectives on
665 evolution in Bromeliaceae. *Botanical Journal of the Linnean Society* 181, 305-322.

666 Pittendrigh, C.S. (1948) The bromeliad-*Anopheles*-malaria complex in Trinidad. I- The bromeliad
667 flora. *Evolution* 2, 58-89.

668 Pockman, W., Sperry, J. (2000) Vulnerability to xylem cavitation and the distribution of the Sonoran
669 desert vegetation. *American Journal of Botany* 87, 1287-1299.

670 Poorter, H., Lambers, H. & Evans, J.R. (2014) Trait correlation networks: a whole-plant perspective
671 on the recently criticized leaf economic spectrum. *New Phytologist* 201, 378-382.

672 Prado, K., Boursiac, Y., Tournaire-Roux, C., Monneuse, J.-M., Postaire, O., Da Ines, O., Schäffner, A.R.,
673 Hem, S., Santoni, V. & Maurel, C. (2013) Regulation of *Arabidopsis* leaf hydraulics involves light-
674 dependent phosphorylation of aquaporins in veins. *Plant Cell* 25, 1029-1039.

675 Reich, P.B., Ellsworth, D.S., Walters, M.B., Vose, J.M., Gresham, C., Volin, J.C &, Bowman, W.D.
676 (1999) Generality of leaf trait relationships: a test across six biomes. *Ecology* 80, 1955-1969.

677 Reich, P.B., Walters, M.B. & Ellsworth, D.S. (1997) From tropics to tundra: global convergence in
678 plant functioning. *Proceedings of the National Academy of Sciences of the USA* 94, 13730-13734.

679 Ripley, B.S., Abraham, T., Klak, C. & Cramer, M.D. (2013). How succulent leaves of Aizoaceae avoid
680 mesophyll conductance limitations of photosynthesis and survive drought. *Journal of Experimental*
681 *Botany* 64, 5485-5496

682 Rull, V. (2011) Neotropical biodiversity: timing and potential drivers. *Trends in Ecology & Evolution*
683 26, 508-513.

684 Sack, L., Pasquet-Kok, J. & Nicotra, A. (2011) *Leaf pressure-volume curve parameters* [WWW
685 document] URL http://prometheuswiki.publish.csiro.au/tiki-index.php?page=Leaf+pressure-
686 volume+curve+parameters [accessed 14 April 2014]

687 Sack, L. & Scoffoni, C. (2012) Measurement of leaf hydraulic conductance and stomatal conductance
688 and their responses to irradiance and dehydration using the evaporative flux method (EFM). *Journal*
689 *of Visualized Experiments* e4179.

690 Sack, L., Scoffoni, C., John, G.P., Poorter, H., Mason, C.M., Mendez-Alonso, R. & Donovan, L.A. (2013)
691 How do leaf veins influence the worldwide leaf economic spectrum? Review and synthesis. *Journal*
692 *of Experimental Botany* 64, 4053-4080.

693 Sade, N., Shatil-Cohen, A., Attia, Z., Maurel, C., Boursiac, Y., Kelly, G., Granot, D., Yaaran, A., Lerner,
694 S. & Moshelion, M. (2014) The role of plasma membrane aquaporins in regulating the bundle
695 sheath-mesophyll continuum and leaf hydraulics. *Plant Physiology* 166, 1609-1620.

696 Scoffoni, C., Albuquerque, C., Brodersen, C.R., Townes, S.V., John, G.P., Bartlett, M.K., Buckley, T.N.,
697 McElrone, A.J. & Sack, L. (2017) Outside-xylem vulnerability, not xylem embolism, controls leaf
698 hydraulic decline during dehydration. *Plant Physiology* doi: http://dx.doi.org/10.1104/pp.16.01643

699 Scoffoni, C., Albuquerque, C., Brodersen, C.R., Townes, S.V., John, G.P., Cochard, H., Buckley, T.N.,
700 McElrone, A.J. & Sack, L. (2016b) Leaf vein xylem conduit diameter influences susceptibility to
701 embolism and hydraulic decline. *New Phytologist* doi: 10.1111/nph.14256

702 Scoffoni, C., Chatelet, D.S., Pasquet-Kok, J., Rawls, M., Donoghue, M.J., Edwards, E.J. & Sack, L.
703 (2016a) Hydraulic basis for the evolution of photosynthetic productivity. *Nature Plants* e16072.

704 Scoffoni, C., McKown, A., Rawls, M. & Sack, L. (2012) Dynamics of leaf hydraulic conductance with
705 water status: quantification and analysis of species differences under steady-state. *Journal of*
706 *Experimental Botany* 63, 643-658.

707 Scoffoni, C., Rawls, M., McKown, A., Cochard, H. & Sack, L. (2011) Decline of leaf hydraulic
708 conductance with dehydration: relationship to leaf size and venation architecture. *Plant Physiology*
709 156, 832-843.

710 Scoffoni, C., Vuong, C., Diep, S., Cochard, H. & Sack, L. (2014) Leaf shrinkage with dehydration:
711 coordination with hydraulic vulnerability and drought tolerance. *Plant Physiology* 164, 1772-1788.

712 Shatil-Cohen, A., Attia, Z. & Moshelion, M. (2011) Bundle-sheath cell regulation of xylem-mesophyll
713 water transport via aquaporins under drought stress: a target of xylem-borne ABA? *Plant Journal* 67,
714 72-80.

715 Silvestro, D., Zizka, G. & Schulte, K. (2014) Disentangling the effects of key innovations on the
716 diversification of Bromelioideae (Bromeliaceae). *Evolution* 68, 163-175.

717 Smith, J.A.C. & Heuer, S. (1981) Determination of the volume of intercellular spaces in leaves and
718 some values for CAM plants. *Annals of Botany* 48, 915-917.

719 Tomlinson, P.B. (1969) *Anatomy of the Monocotyledons. III: Commelinales-Zingiberales*. Oxford, UK:
720 Clarendon Press.

721 Unger, F. (1854) Beiträge zur Physiologie der Pflanzen. I. Bestimmung der in den Interzellulargängen
722 der Pflanzen enthaltenen Luftmenge. *Königliche Akadamie der Wissenschaften*: *Mathamatik-*
723 *Naturwissenschaften* 12, 367-378.

724 Vasseur, F., Violle, C., Enquist, B.J., Granier, C. & Vile, D. (2012) A common genetic basis to the origin
725 of the leaf economics spectrum and metabolic scaling allometry. *Ecology Letters* 15, 1149-1157.

726 Villagra, M., Campanello, P.I., Bucci, S.J. & Goldstein, G. (2013) Functional relationships between leaf
727 hydraulics and leaf economic traits in response to nutrient addition in subtropical trees. *Tree*
728 *Physiology* 33, 1308-1318.

729 Wagner, J. & Larcher, W. (1981) Dependence of CO_2 gas exchange and acid metabolism of the alpine
730 CAM plant *Sempervivum montanum* on temperature and light. *Oecologia* 50, 88-93.

731 Wheeler, J.K., Sperry, J.S., Hacke. U.G. & Hoang, N. (2005) Inter-vessel pitting and cavitation in
732 woody Rosaceae and other vesselled plants: a basis for a safety versus efficiency trade-off in xylem
733 transport. *Plant, Cell & Environment* 28, 800-812.

734 Wright, I.J., Reich, P.B., Cornelissen, J.H.C., Falster, D.S., Garnier, E., Hikosaka, K., … & Westoby, M.
735 (2005) Assessing the generality of global leaf trait relationships. *New Phytologist* 166, 485-496.

736 Wright, I.J., Reich, P.B., Westoby, M., Ackerly, D.D., Baruch, Z., Bongers, F., … & Villar, R. (2004) The
737 worldwide leaf economics spectrum. *Nature* 428, 821-827.

738 Zotz, G. & Hietz, P. (2001) The physiological ecology of vascular epiphytes: current knowledge, open
739 questions. *Journal of Experimental Botany* 52, 2067-2078.

740

741

742

743

744

745

746

747 **TABLES**

748

749 Table 1. Significant correlations between species-mean leaf trait values across all bromeliad species
750 samples (n = 50). Trait definitions: A_{max} = maximum photosynthetic capacity (μmol m^{-2} s^{-1}); N_{leaf} = leaf
751 nitrogen content (%); P_{leaf} = leaf phosphorus content (%); LMA; VED = vein-epidermis distance (μm);
752 IVD = interveinal distance (μm); $K_{leafmax}$ = maximum leaf hydraulic conductance (mmol m^{-2} s^{-1} MPa^{-1});
753 R_D = dark respiration rate (μmol m^{-2} s^{-1}); R_L = light respiration rate (μmol m^{-2} s^{-1}); ε = bulk elastic
754 modulus (MPa); P_{50L} = leaf water potential at 50% loss of $K_{leafmax}$ (MPa); Ψ_{tlp} = leaf water potential at
755 turgor loss point (MPa); SD = stomatal density (mm^{-2}); g_{smax} = maximum stomatal conductance (mol
756 m^{-2} s^{-1}); IAS = intercellular air space fraction (%); C_{FT} = hydraulic capacitance at full turgor (mol m^{-2}
757 MPa^{-1}).

Trait 1	**Trait 2**	**Sign of correlation**	r^2	p
A_{max}	N_{leaf}	+	0.31	< 0.001
A_{max}	P_{leaf}	+	0.49	< 0.001
A_{max}	LMA	-	0.10	0.015
N_{leaf}	P_{leaf}	+	0.17	0.002
A_{max}	R_D	+	0.63	< 0.001
A_{max}	R_L	+	0.48	< 0.001
R_L	R_D	+	0.74	< 0.001
P_{leaf}	R_D	+	0.69	< 0.001
P_{leaf}	R_L	+	0.51	< 0.001
LMA	VED	+	0.39	< 0.001
LMA	IAS	-	0.56	< 0.001
VED	IAS	-	0.63	< 0.001
IVD	VED	+	0.59	< 0.001
A_{max}	SD	+	0.44	< 0.001
$K_{leafmax}$	SD	+	0.70	< 0.001
R_D	SD	+	0.38	< 0.001
R_L	SD	+	0.26	< 0.001
E	SD	+	0.62	< 0.001
P_{50L}	SD	-	0.42	< 0.001
Ψ_{tlp}	SD	-	0.31	< 0.001
A_{max}	g_{smax}	+	0.57	< 0.001
A_{max}	IAS	+	0.39	< 0.001
A_{max}	$K_{leafmax}$	+	0.87	< 0.001
$K_{leafmax}$	g_{smax}	+	0.80	< 0.001
$K_{leafmax}$	P_{50L}	-	0.42	< 0.001
P_{50L}	Ψ_{tlp}	+	0.93	< 0.001

C_{FT}	ε	-	0.29	< 0.001

782 Table 2. Mean values (± standard error of the mean) for leaf traits by functional type.

Trait	C_3 terrestrials (*n* = 10)	CAM terrestrials (*n* = 7)	C_3 tank-epiphytes (*n* = 14)	CAM tank-epiphytes (*n* = 10)	CAM atmospheric epiphytes (*n* = 9)
A_{max} ($\mu mol\ m^{-2}\ s^{-1}$)	4.84 ± 0.36	1.47 ± 0.30	3.71 ± 0.18	2.19 ± 0.27	0.86 ± 0.05
N_{leaf} (%)	1.14 ± 0.10	0.80 ± 0.07	1.10 ± 0.09	0.83 ± 0.09	0.83 ± 0.04
PNUE (A_{max}/N_{leaf})	2.66 ± 0.74	0.58 ± 0.09	5.91 ± 0.92	3.45 ± 0.98	0.63 ± 0.04
LMA ($g\ m^{-2}$)	236.34 ± 32.39	302.96 ± 20.95	75.86 ± 8.36	151.52 ± 18.75	173.20 ± 10.60
g_{smax} ($mol\ m^{-2}\ s^{-1}$)	0.175 ± 0.019	0.018 ± 0.002	0.099 ± 0.008	0.012 ± 0.001	0.007 ± 0.001
iWUE (A_{max}/g_s)	32.04 ± 4.75	85.11 ± 21.13	40.89 ± 3.44	200.18 ± 27.55	130.79 ± 11.69
P_{leaf} (%)	0.021 ± 0.001	0.012 ± 0.001	0.011 ± 0.001	0.010 ± 0.001	0.004 ± 0.001
C:N	35.23 ± 3.83	56.28 ± 7.39	44.06 ± 3.77	56.51 ± 5.95	53.65 ± 3.95
R_L ($\mu mol\ m^{-2}\ s^{-1}$)	0.42 ± 0.01	0.25 ± 0.02	0.28 ± 0.01	0.28 ± 0.02	0.24 ± 0.02
R_D ($\mu mol\ m^{-2}\ s^{-1}$)	0.66 ± 0.01	0.35 ± 0.02	0.42 ± 0.02	0.37 ± 0.02	0.31 ± 0.02
$\delta^{13}C$ (‰)	-26.13 ± 0.78	-15.07 ± 0.57	-25.62 ± 0.41	-16.19 ± 0.75	-15.18 ± 0.27
VED (µm)	289.08 ± 34.61	404.21 ± 15.49	154.74 ± 11.45	362.50 ± 19.72	421.39 ± 16.27
IVD (µm)	311.06 ± 17.45	320.86 ± 26.14	253.09 ± 11.09	322.71 ± 8.36	336.63 ± 6.41
$K_{leafmax}$ ($mmol\ m^{-2}\ s^{-1}\ MPa^{-1}$)	3.64 ± 0.47	0.05 ± 0.02	0.98 ± 0.10	0.18 ± 0.03	0.02 ± 0.002
Ψ_{tlp} (MPa)	-1.47 ± 0.03	-1.07 ± 0.06	-1.01 ± 0.04	-1.07 ± 0.08	-0.86 ± 0.04
ε (MPa)	13.45 ± 1.58	2.86 ± 0.35	6.35 ± 0.65	5.96 ± 0.44	3.86 ± 0.93
C_{FT} ($mol\ m^{-2}\ MPa^{-1}$)	7.32 ± 1.01	10.50 ± 1.06	4.30 ± 0.34	5.09 ± 0.39	10.90 ± 1.13

P_{50S} (MPa)	-0.47 ± 0.01	-0.47 ± 0.02	-0.36 ± 0.01	-0.49 ± 0.04	-0.37 ± 0.006
P_{50L} (MPa)	-1.49 ± 0.05	-1.07 ± 0.07	-0.98 ± 0.03	-1.10 ± 0.08	-0.87 ± 0.05
SD (mm^{-2})	165.74 ± 56.46	11.24 ± 1.34	30.15 ± 2.52	23.40 ± 4.15	3.75 ±0.16
IAS (%)	8.47 ± 1.64	6.03 ± 0.36	13.08 ± 0.85	8.63 ± 0.67	6.02 ± 0.33

FIGURE LEGENDS

Figure 1. Examples of the functional types in the Bromeliaceae: a) *Fascicularia bicolor* (Ruiz & Pav.) Mez, C_3 terrestrial; b) *Deuterocohnia brevifolia* (Griseb.) M.A.Spencer & L.B.Sm., CAM terrestrial; c) *Vriesea splendens* (Brongn.) Lem., C_3 tank-epiphyte; d) *Aechmea fendleri* André ex Mez, CAM tank-epiphyte; e) *Tillandsia ionantha* Planch., CAM atmospheric epiphyte.

Figure 2. Examples of transverse leaf cross sections from species of different functional types showing key anatomical parameters. a) *Puya chilensis* (C_3 terrestrial); b) *Bromelia humilis* (CAM terrestrial); c) *Vriesea splendens* (C_3 tank-epiphyte); d) *Aechmea fasciata* (CAM tank-epiphyte); e) *Tillandsia caput-medusae* (CAM atmospheric). Bars = 200 μm.

Figure 3. a) Bioclimatic distribution of 46/50 of the bromeliad species used in this investigation across the biome space defined by mean annual precipitation (MAP) and mean annual temperature (MAT; Whittaker, 1975). Open squares: C_3 terrestrials; filled squares: CAM terrestrials; open triangles: C_3 tank-epiphytes; filled triangles: CAM tank-epiphytes; filled circles: CAM atmospheric epiphytes. b) Location of all 50 bromeliad species in the leaf economic spectrum (LES) trait space defined by leaf mass per unit area (LMA; g m^{-2}) versus leaf N content (%; Wright et al., 2004). Grey background points are taken from the Global Plant Trait Network (GLOPNET) Database, with bromeliad species plotted as in a).

Figure 4. Leaf water potential at 50% loss stomatal conductance (P_{50S}) by functional type. Boxes show median values and interquartile range (IQR); whiskers indicate full range of values.

Figure 5. Percent loss of conductance (PLC) in K_{leaf} and g_s as functions of declining Ψ_{leaf} for five bromeliad species of different functional types: a) *Pitcairnia integrifolia*, C_3 terrestrial; b) *Ananas comosus*, CAM terrestrial; c) *Guzmania lingulata*, C_3 tank-epiphyte; d) *Aechmea aquilega*, CAM tank-epiphyte; e) *Tillandsia stricta*, CAM atmospheric. Filled circles show mean values of PLC for K_{leaf} relative to $K_{leafmax}$; open circles show mean values of PLC for g_s relative to g_{smax}. Means are based on five biological replicates per species; error bars indicate ± standard error of the mean. Solid lines

show fitted curves for K_{leaf}; short dashed lines show fitted curves for g_s. Intersections of the fitted curves with the straight line at PLC = 50% represent P_{50L} and P_{50S}.

Figure 6. Leaf economic, hydraulic and anatomical trait relationships in the bromeliads. Main plots show raw data, insets show log-transformed data with linear regression lines. a) A_{max} vs. N_{leaf}; b) P_{leaf} vs. N_{leaf}; c) A_{max} vs. LMA; d) A_{max} vs. IAS; e) A_{max} vs. $K_{leafmax}$; f) g_{smax} vs. $K_{leafmax}$; g) $K_{leafmax}$ vs. SD; h) $K_{leafmax}$ vs. absolute P_{50L}; i) Ψ_{tlp} vs. absolute P_{50L}; j) C_{FT} vs. ε; k) VED vs. IVD; l) R_D vs. R_L. Open squares: C_3 terrestrials; filled squares: CAM terrestrials; open triangles: C_3 tank-epiphytes; filled triangles: CAM tank-epiphytes; filled circles: CAM atmospheric epiphytes. Correlations are presented in Table 1.

Figure 7. a) Relationship between absolute values of K_{leaf} and g_s at P_{50L}; b) relationship between absolute values of K_{leaf} and g_s at P_{50S}; c) relationship between absolute P_{50L} and absolute value of K_{leaf} at P_{50L}; d) relationship between $K_{leafmax}$ and P_{50L}. Main plots show values calculated from K_{leaf}-Ψ_{leaf} and g_s-Ψ_{leaf} curve-fitting, insets show log-transformed values with linear regression lines. Open squares: C_3 terrestrials; filled squares: CAM terrestrials; open triangles: C_3 tank-epiphytes; filled triangles: CAM tank-epiphytes; filled circles: CAM atmospheric epiphytes.

Figure 8. Biplots of first two principal components in an analysis of variation in 20 continuous traits across all 50 bromeliad species used in this investigation showing a) trait loadings and b) species loadings plotted by functional types. Open squares: C_3 terrestrials; filled squares: CAM terrestrials; open triangles: C_3 tank-epiphytes; filled triangles: CAM tank-epiphytes; filled circles: CAM atmospheric epiphytes.

Figure 9. Major trends in ecophysiological characteristics associated with transitions between functional types as suggested by data collected in this investigation.

862 **FIGURES**

863 Figure 1. (colour)

864

865

866

867

868

869

870

871 Figure 2.

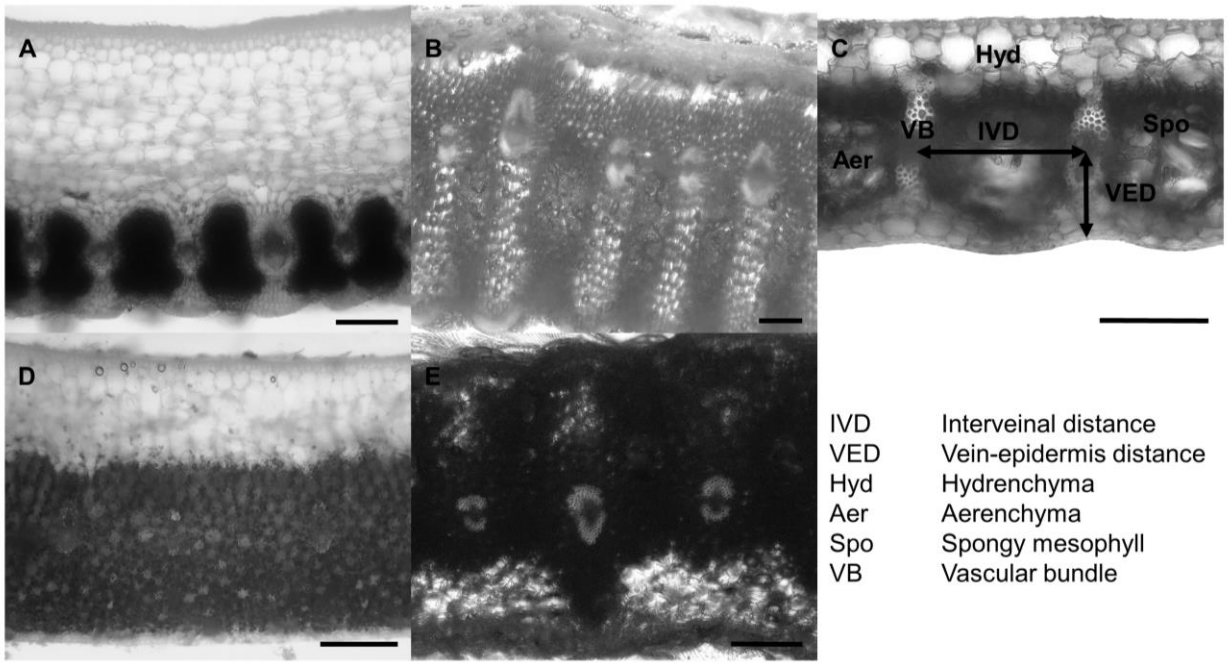

872

873

874

875

876

877

878

879

880

881

882

883

884

885

886

887

888

889

890

891 Figure 3.

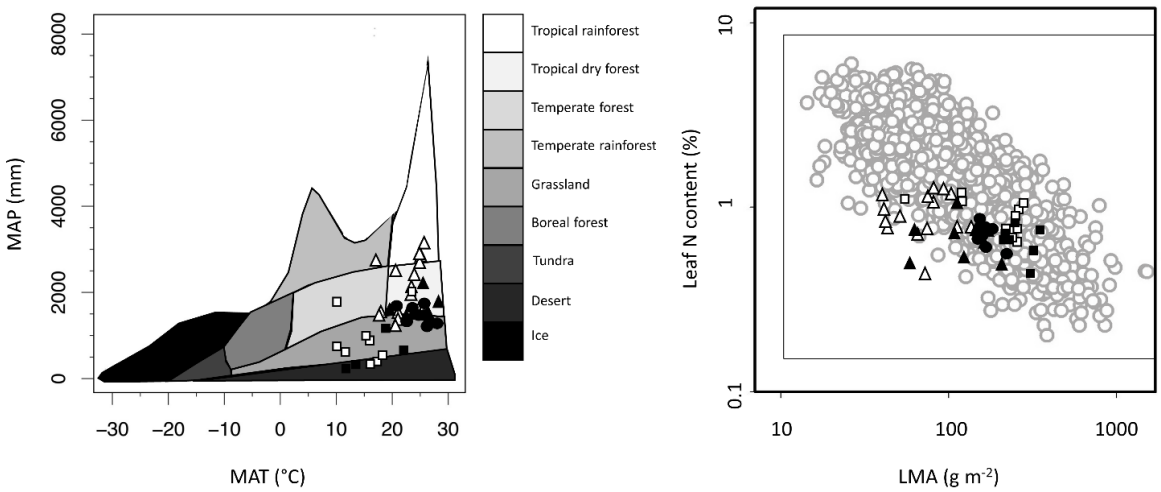

892

893

894

895

896

897

898

899

900

901

902

903

904

905

906

907

908

909

910 Figure 4.

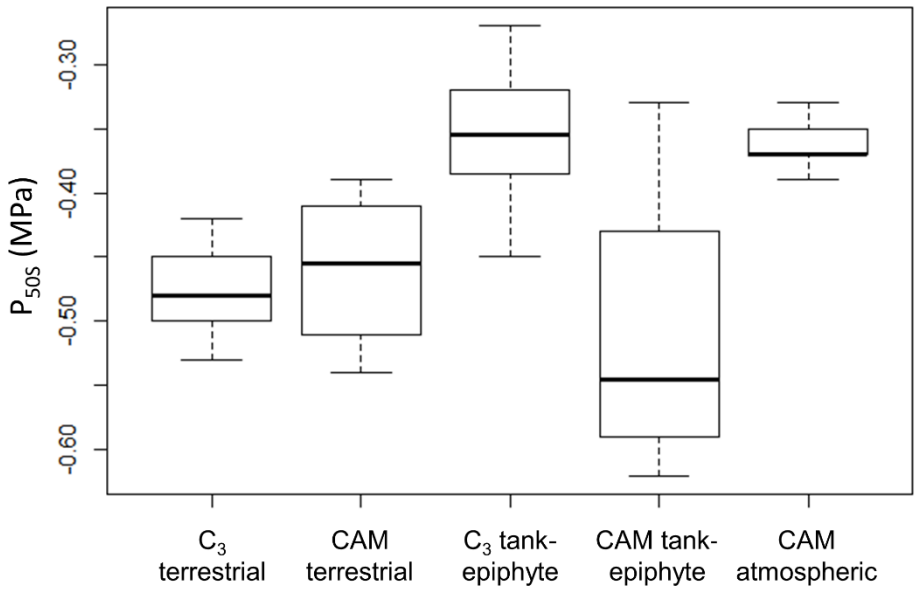

911

912

913

914

915

916

917

918

919

920

921

922

923

924

925

926

927 Figure 5.

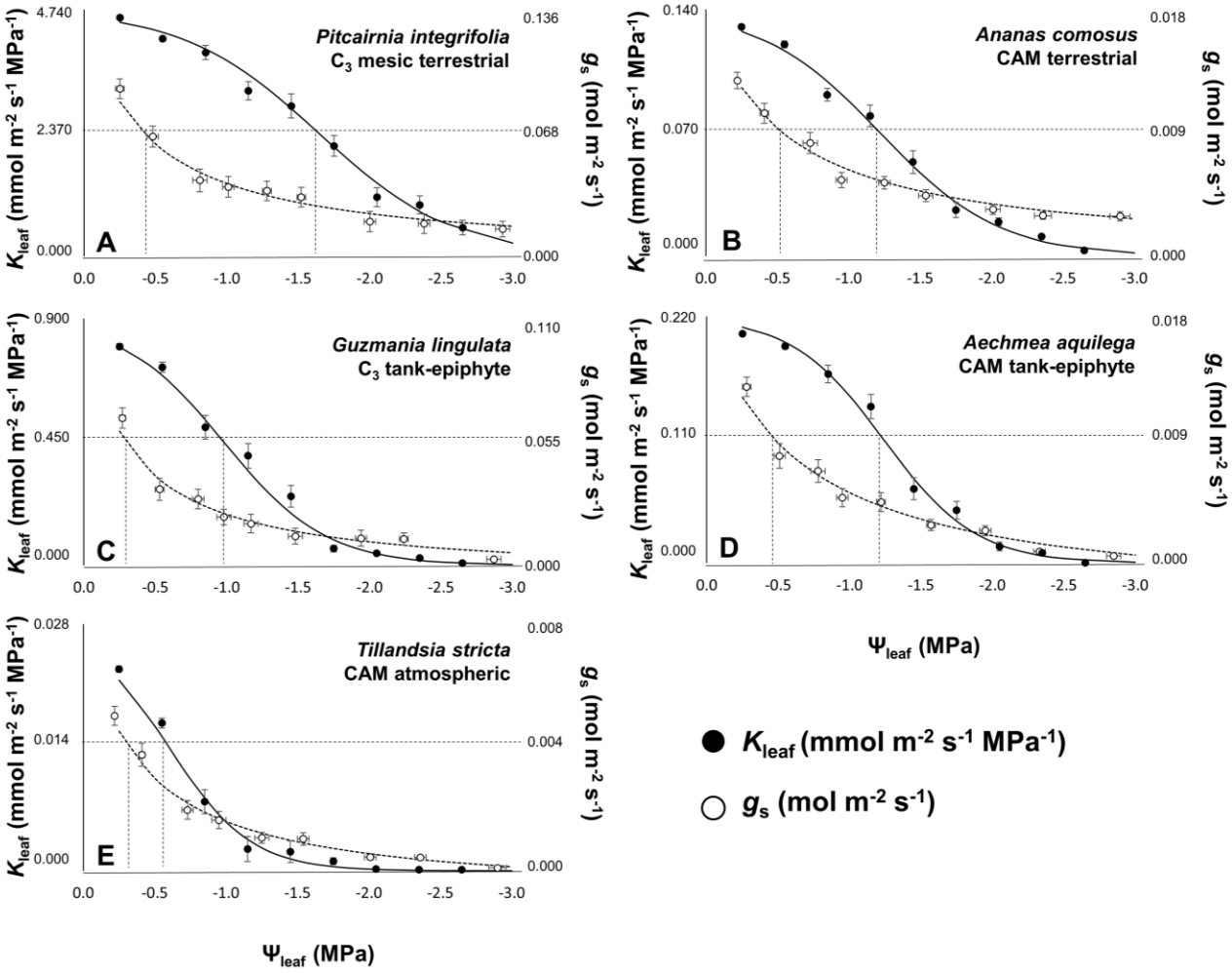

928

929

930

931

932

933

934

935

936

937

938 Figure 6.

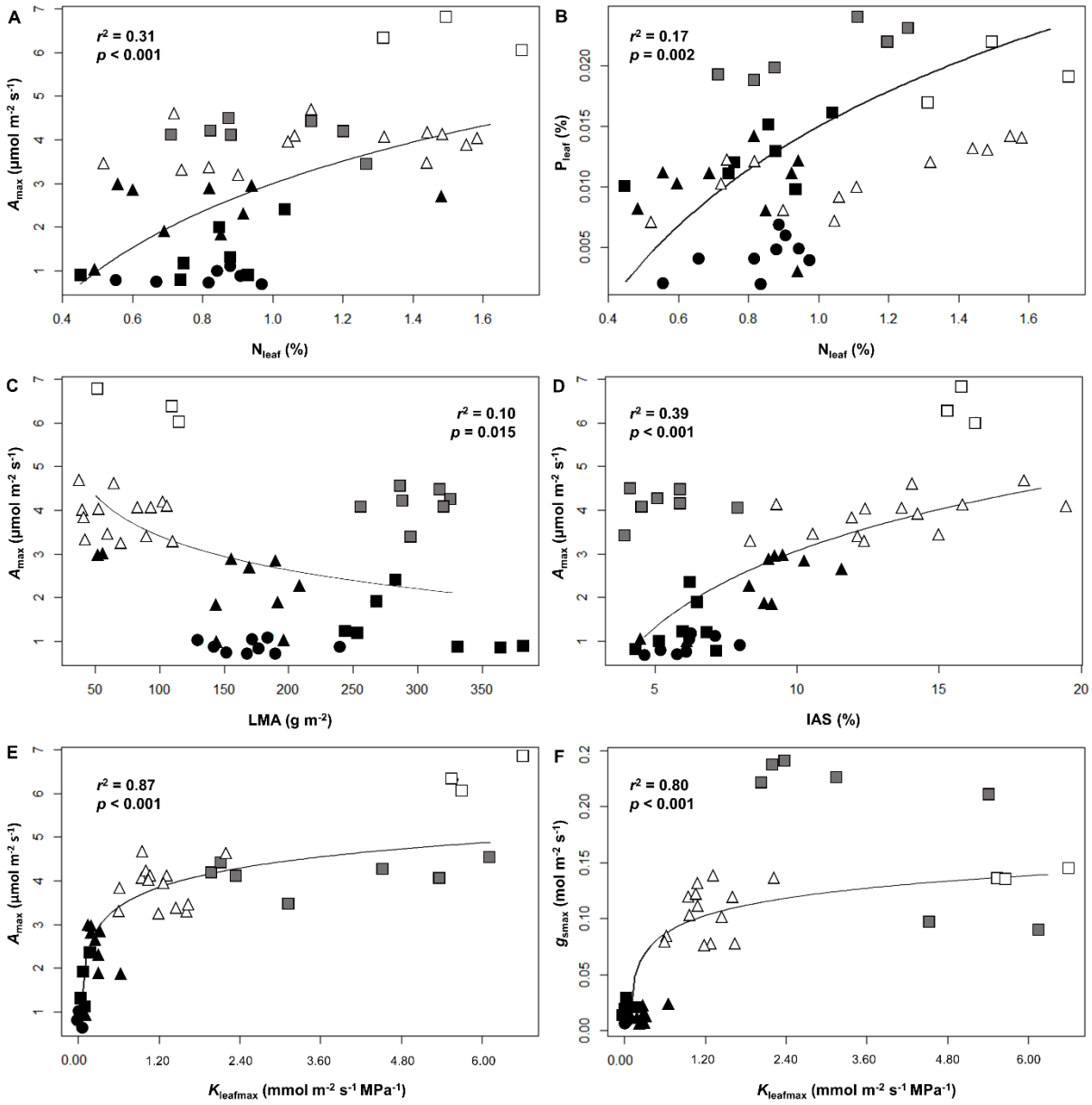

939

940

941

942

943

944

945

946

947 Figure 6 (cont.)

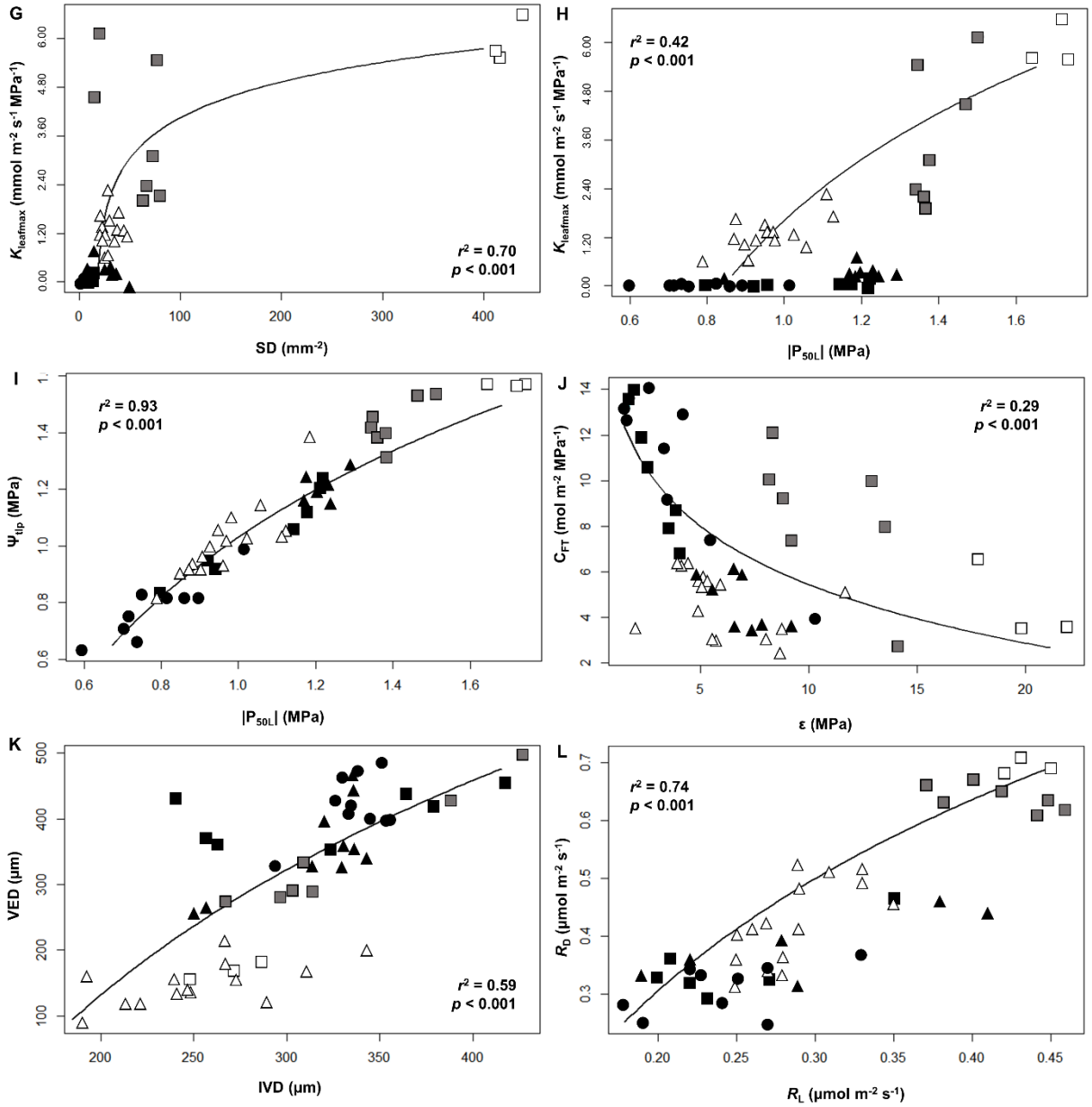

948

949

950

951

952

953

954

Figure 7.

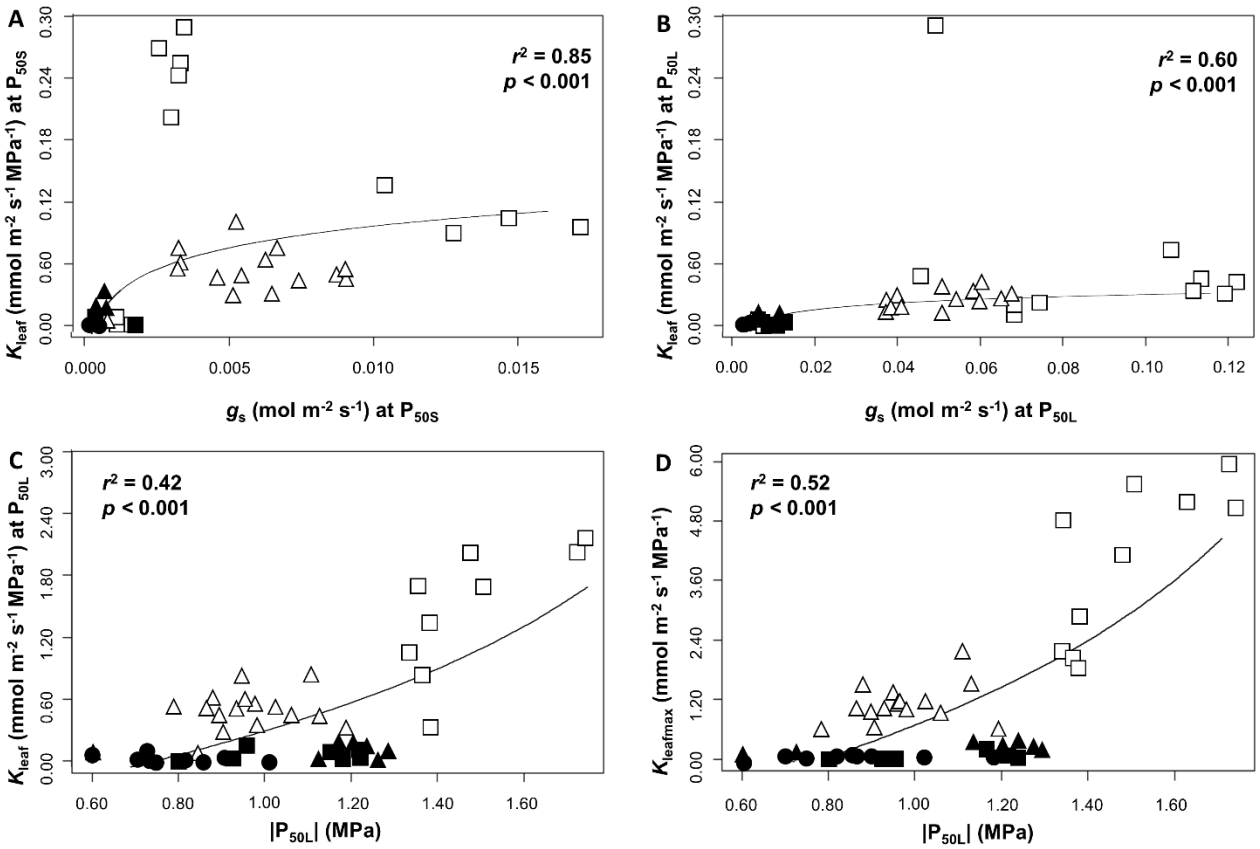
A
r^2 = 0.85
p < 0.001
K_{leaf} (mmol m^{-2} s^{-1} MPa^{-1}) at P_{50S}
g_s (mol m^{-2} s^{-1}) at P_{50S}
B
r^2 = 0.60
p < 0.001
K_{leaf} (mmol m^{-2} s^{-1} MPa^{-1}) at P_{50L}
g_s (mol m^{-2} s^{-1}) at P_{50L}
C
r^2 = 0.42
p < 0.001
K_{leaf} (mmol m^{-2} s^{-1} MPa^{-1}) at P_{50L}
|P_{50L}| (MPa)
D
r^2 = 0.52
p < 0.001
$K_{leafmax}$ (mmol m^{-2} s^{-1} MPa^{-1})
|P_{50L}| (MPa)

969 Figure 8.

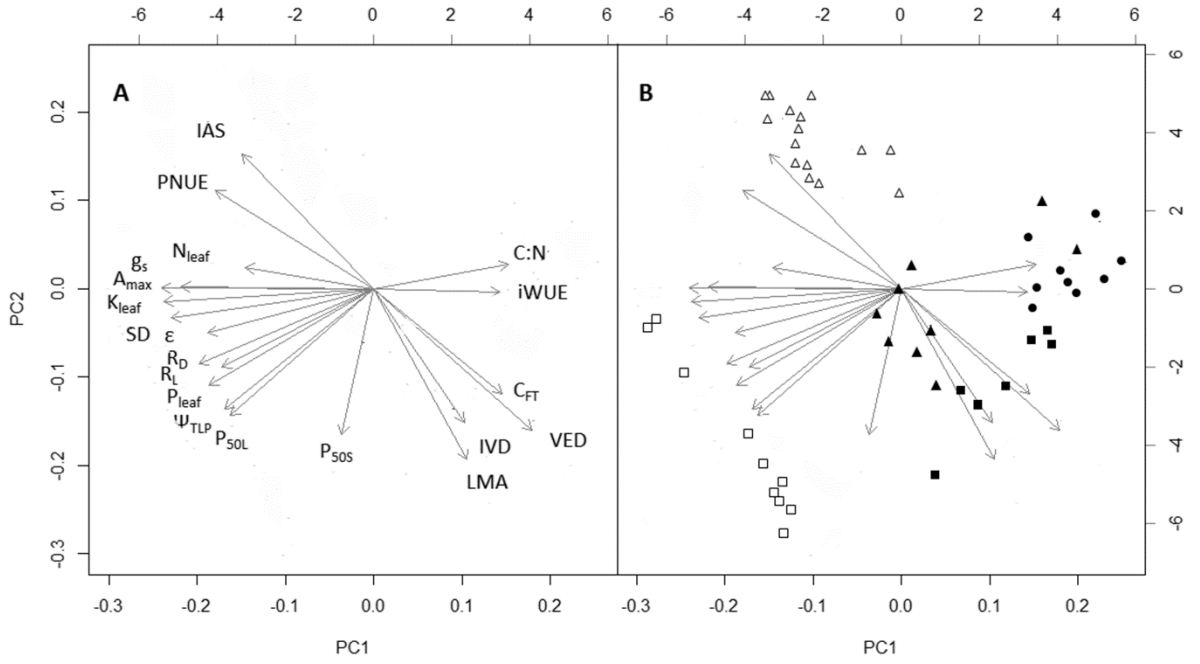

970

971

972

973

974

975

976

977

978

979

980

981

982

983

984

985 Figure 9.

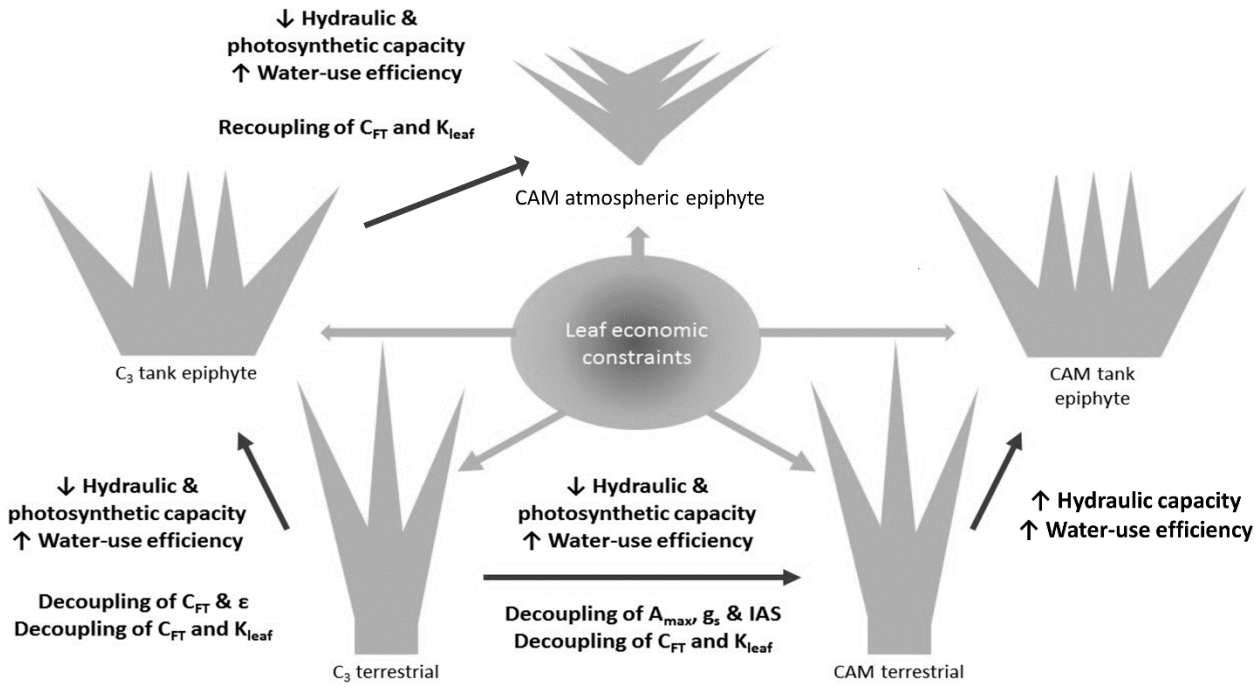

986